

RESEARCH ARTICLE | AUGUST 19 2019

Simulation of the two-dimensional Rayleigh-Taylor instability problem by using diffuse-interface model

Special Collection: [2019 Mathematical Physics](#)

Saher Akmal Khan; Abdullah Shah



AIP Advances 9, 085312 (2019)

<https://doi.org/10.1063/1.5100791>

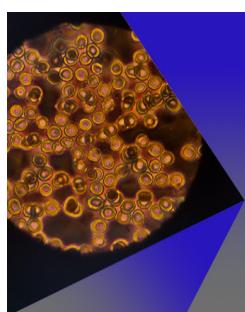


[View
Online](#)



[Export
Citation](#)

CrossMark



AIP Advances

Special Topic: Medical Applications
of Nanoscience and Nanotechnology

Submit Today!

 AIP
Publishing

Simulation of the two-dimensional Rayleigh-Taylor instability problem by using diffuse-interface model

Cite as: AIP Advances 9, 085312 (2019); doi: 10.1063/1.5100791

Submitted: 20 April 2019 • Accepted: 7 August 2019 •

Published Online: 19 August 2019



View Online



Export Citation



CrossMark

Saher Akmal Khan^{a)} and Abdullah Shah^{b)}

AFFILIATIONS

Department of Mathematics, COMSATS University Islamabad, 44000, Pakistan

^{a)}Electronic mail: saher.akmal.khan@gmail.com

^{b)}Electronic mail: abdullah_shah@comsats.edu.pk

ABSTRACT

The purpose of this paper is to simulate a two-dimensional Rayleigh-Taylor instability problem using the diffuse-interface formulation of the incompressible Navier-Stokes equations. The governing equations consist of a system of coupled nonlinear partial differential equations for conservation of mass, momentum and phase transport. The Boussinesq approximation is introduced in the momentum equation to relax the complexity of variable density formulation. Due to the simplicity, this approximation can be used for small density variations in simulating two-phase flows. The numerical scheme is based on an artificial compressibility formulation with a finite difference scheme for the space discretization. To validate the method, the penetration of a heavier fluid into the lighter one is computed and illustrated graphically.

© 2019 Author(s). All article content, except where otherwise noted, is licensed under a Creative Commons Attribution (CC BY) license (<http://creativecommons.org/licenses/by/4.0/>). <https://doi.org/10.1063/1.5100791>

15 July 2023 18:51:49

I. INTRODUCTION

In two-phase flow, the dynamic variables like the velocity, viscosity, pressure, and density are normally used to explain the movement of fluids. The density is used to determine the compressibility of the two-phase fluid flow. Because of the multifaceted nature of density change in the fluids, couple of suppositions were taken to diminish the level of the intricacy. One of the presumptions among other is, the Boussinesq approximation^{1,2} which is utilized for buoyancy-driven flows.

Rayleigh-Taylor (RT) instability is a phenomena in which heavier fluid is superposed over a lighter one in a gravitational field where the fluid interface is unstable. Any perturbation of this interface will in general develop with time, exhibiting the penetration of both heavier and lighter fluids into one another. The RT instability due to the gravitational field was initially proposed by Rayleigh³ and subsequently has been applied to all fluids by Taylor.⁴ This instability has been applied to a wide range of problems, including the mushroom clouds like volcanic eruptions and atmospheric nuclear explosions, plasma fusion reactors instability and inertial confinement fusion,⁵ Oceanographic⁶ and supernova explosions⁷ in which the

expanding core gas is accelerated into a denser shell gas. Several numerical techniques have been suggested to study the relatively short time RT instability phenomena including boundary integral methods,⁸ front tracking methods,^{9,10} volume of fluid methods,^{11–13} level set methods^{14,15} and phase-field methods.^{16–19} Most of the results presented were for relatively short time experiments.²⁷ However, the long time simulations of the RT instability can be applied to a gravity separator to separate oil and water. Complete separation time is one of the crucial factors in designing the separator.¹⁸

In this work, we perform the long time evolutions of RT instability resulting in an equilibrium state by implementing the diffuse-interface method developed by Shah and Yuan.²⁰ The computed results are compared with one found in literature¹⁸ and a good agreement is observed qualitatively.

The diffuse-interface method is an algorithm for solving the two-phase flow problems in such a way that a diffuse interface replaces the sharp fluid interface with non-zero thickness in the transition layer. It provides a powerful tool for the evolution of moving interface and handling of the topological changes. In this method, an interface as a finite volumetric zone across which the physical properties like density and viscosity varies steeply and continuously. The

location and shape of the interface at each time instant is determined by minimizing the free energy of the system without using interface boundary condition explicitly.²³ The idea of a diffuse-interface was first considered by van der Waals in the late nineteenth century.²² J. W. Gibbs treated the thermodynamics of diffuse-interface changes in Ref. 18. The diffuse-interface method uses two distinct values for the phase variable ϕ (for instance +1 and -1) in each of the phases while smoothly change between both values in the region around the interface, which is diffused with a finite thickness. The initial profile of the RT instability with diffuse-interface approach is given in Fig. 1(a), where a heavy fluid is superposed over a light fluid in a gravitational field. Any perturbation of this interface tends to grow with time which is shown in Fig. 1(b).

In this study, we considered a system consisting of two incompressible fluids having different densities, ρ_1 and ρ_2 , such that, $\rho_2 > \rho_1$, with the denser fluid is placed above the less dense one. The initial perturbation is given by $\phi(x, 0) = \tanh(\frac{y-2-0.1\cos(2\pi x)}{\sqrt{2}\eta})$, where η is the interfacial width. The flow configuration remains stable when no gravity is acting on it and the density variation is not too large. However, in the presence of gravitational force, the heavier fluid sink and the lighter fluid starts rising causing the interface to distort because heavier fluid will keep trying to sink while the lighter fluid rises with disturbance in flow regime as shown in the Fig. 1(b).

A. The diffuse-interface method

Let Ω be a domain filled with two immiscible fluids of different densities separated by an interface as shown in Fig. 1(a). The phase function $\phi(x, t)$ with $x \in \Omega$ assumes distinct values $\phi = 1$ with

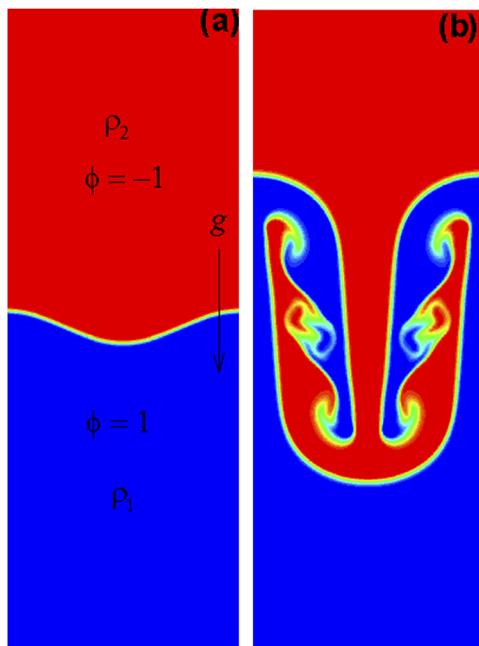


FIG. 1. Geometry of the Rayleigh-Taylor instability problem. The initial perturbation is given by $\phi(x, 0) = \tanh(y-2-0.1\cos(2\pi x)/\sqrt{2}\eta)$ at $t = 0$ in figure 1(a) and its simulation at time $t = 0.9$ in figure 1(b).

density ρ_1 in one fluid and $\phi = -1$ in the other fluid with ρ_2 having smooth change in the interfacial region with thickness η . The elastic mixing free-energy of two-component fluids can be expressed by the Ginzburg-Landau free-energy functional of the form:

$$F(\phi, \nabla\phi) = \int_{\Omega} \left(\frac{1}{2} |\nabla\phi|^2 + \frac{1}{4\eta^2} (\phi^2 - 1)^2 \right) dx, \quad (1)$$

where the constant η is an artificial thickness for the diffusive interface. The gradient term for ϕ in equation (1) leads to a diffuse liquid-liquid interface, a feature observed both experimentally and numerically,^{28,29} while the latter term is a double-well potential taken as $\frac{1}{4\eta^2}(\phi^2 - 1)^2 = 0$, gives the separated phases as pure components ($|\phi| = 1$). The evolution of ϕ is governed by the Allen-Cahn equation:²⁴

$$\phi_t + (\mathbf{u} \cdot \nabla)\phi = -\gamma \frac{\delta F}{\delta \phi} = \gamma(\Delta\phi - f(\phi)). \quad (2)$$

with

$$\frac{d}{dt} \int_{\Omega} \phi dx = 0, \quad (3)$$

Here, $\delta F/\delta\phi$ represents the variational derivative of the energy functional $F(\phi, \nabla\phi)$ with respect to ϕ , $f(\phi) = \frac{\phi(\phi^2-1)}{\eta^2}$ and γ is the elastic relaxation time-scale of the two fluids.

The Allen-Cahn equation is a second-order stiff nonlinear parabolic partial differential equation which was originally introduced by Allen and Cahn to describe the phase separation in binary alloys and motion of antiphase boundaries in crystalline solids. Nowadays, this equation is being used in many moving boundary problems in fluid dynamics, materials science and image processing through a phase-field approach. With the Allen-Cahn equation, one can deal with the evolution of arbitrary morphologies and complex micro-structures without tracking the position of moving interface explicitly. The Allen-Cahn equation has been used to model various phenomena in nature, such as impact of a droplet on a solid surface, image segmentation, the motion by mean curvature flow, crystal and tumor growth etc. In particular, it has become a fundamental equation for the diffuse interface method that has been developed to study phase transitions and interfacial dynamics in multi-phase flows. However, due to the non-conserved nature of the Allen-Cahn equation, the mass conservation is a big issue in using this equation. To keep the mass conserve, either we need to solve the conservative Allen-Cahn equation³⁰ or the 4th-order Cahn-Hilliard equation.^{31,32} One of the reasons for choosing Allen-Cahn equation is due to its ease in numerical treatment than that of the Cahn-Hilliard type which involves 4th-order differential operator.

B. The Boussinesq approximation model

By adding the Boussinesq approximation term in the momentum equation of the incompressible Navier-Stokes equation for small density variation as follows:

$$\rho_0[u_t + (u \cdot \nabla)u] = -\nabla\tilde{p} + \nabla \cdot \sigma + b(\phi), \quad (4)$$

where \tilde{p} is the pressure that has absorbed $\rho_0 gy$ from original gravity term, σ is the lumped stress tensor that includes the viscous stress tensor and the induced elastic stress tensor and ρ_0 is the background

density treated as constant in the whole flow-field and the difference between the actual density and ρ_0 contributes only to the buoyancy force $b(\phi)$. σ is given by;

$$\sigma = \mu(\phi)[\nabla u + (\nabla u)^t] - \lambda \nabla \phi \otimes \nabla \phi, \quad (5)$$

where, $\mu(\phi) = \frac{1+\phi}{2}\mu_1 + \frac{1-\phi}{2}\mu_2$ is the dynamic viscosity of the mixture, λ is the surface tension coefficient and $(\nabla \phi \otimes \nabla \phi)_{ij} = \nabla_i \phi \nabla_j \phi$ is the usual stress tensor product.

By using the identity,

$$\nabla \cdot (\nabla \phi \otimes \nabla \phi) = \Delta \phi \nabla \phi + \left(\frac{1}{2}|\nabla \phi|^2\right), \quad (6)$$

the momentum equation is further simplified by redefining the pressure term as $p = \tilde{p} + \frac{1}{2}\lambda|\phi|^2$. The buoyancy force with gravitational acceleration g in the negative y -direction is given as $b(\phi) = (0, -g(\rho(\phi) - \rho_0))^T$, (contribution of density is only in buoyancy force terms of momentum equation). By using $\rho(\phi) = \frac{1+\phi}{2}\rho_1 + \frac{1-\phi}{2}\rho_2$, the buoyancy contribution is

$$\begin{aligned} -g(\rho(\phi) - \rho_0) &= -g\left(\frac{1+\phi}{2}\rho_1 + \frac{1-\phi}{2}\rho_2 - \rho_0\right), \\ &= -\frac{g}{2}(\rho_1 + \rho_2 + (\rho_1 - \rho_2)\phi - 2\rho_0) \\ &\approx -\frac{g}{2}(\rho_1 - \rho_2 + (\rho_1 - \rho_2)\phi) \\ &= -g(\rho_1 - \rho_2)\left(\frac{1+\phi}{2}\right). \end{aligned} \quad (7)$$

Here we have assuming $\rho_0 \approx \rho_2$, where ρ_0 is the background density. We restrict ourself to a simpler type of incompressible two-fluid mixture³⁵ with a viscosity constant $\mu_1 = \mu_2 = \mu$.

II. GOVERNING EQUATIONS

The incompressible flows are usually governed by continuity and momentum equations known as the Navier-Stokes equations. These equations are difficult to solve analytically or numerically due to the presence of nonlinear convective terms. To handle this problem Chorin²⁵ in 1967 introduced a method called artificial compressibility method, in which the continuity equation is modified by adding an artificial compressibility factor β in such a way that it vanishes when steady state is reached. With this concept below Eqs. (8), (9), (10) and (11) can be written as:

$$\frac{\partial p}{\partial \tau} + \beta\left(\frac{\partial u}{\partial x} + \frac{\partial v}{\partial y}\right) = 0, \quad (8)$$

$$\begin{aligned} \frac{\partial u}{\partial \tau} + \frac{\partial u}{\partial t} + \frac{\partial(u^2 + p)}{\partial x} + \frac{\partial uv}{\partial y} - \mu\left(\frac{\partial^2 u}{\partial x^2} + \frac{\partial^2 u}{\partial y^2}\right) \\ = -\lambda \frac{\partial \phi}{\partial x} \left(\frac{\partial^2 \phi}{\partial x^2} + \frac{\partial^2 \phi}{\partial y^2}\right), \end{aligned} \quad (9)$$

$$\begin{aligned} \frac{\partial v}{\partial \tau} + \frac{\partial v}{\partial t} + \frac{\partial(v^2 + p)}{\partial y} + \frac{\partial uv}{\partial x} - \mu\left(\frac{\partial^2 v}{\partial x^2} + \frac{\partial^2 v}{\partial y^2}\right) \\ = -\lambda \frac{\partial \phi}{\partial y} \left(\frac{\partial^2 \phi}{\partial x^2} + \frac{\partial^2 \phi}{\partial y^2}\right) - g(\rho_1 - \rho_2)\left(\frac{1+\phi}{2}\right), \end{aligned} \quad (10)$$

$$\begin{aligned} \frac{\partial \phi}{\partial \tau} + \frac{\partial \phi}{\partial t} + \frac{\partial(v\phi)}{\partial y} + \frac{\partial(u\phi)}{\partial x} - \gamma\left(\frac{\partial^2 \phi}{\partial x^2} + \frac{\partial^2 \phi}{\partial y^2}\right) \\ = \gamma(1 - \phi^2)\left(\frac{\phi}{\eta^2} + \xi(t)\right). \end{aligned} \quad (11)$$

The coupled nonlinear system is subject to the initial conditions

$$\mathbf{u}|_{t=0} = \mathbf{u}_0, \quad (12)$$

$$\phi|_{t=0} = \phi_0, \quad (13)$$

and periodic boundary conditions to vertical boundaries and Neumann boundary conditions to the top and bottom domain.

By introducing Lagrange multiplier term $\xi(t)$ in the Allen-Cahn equation that allows to ensure mass conservation.^{33,34} The role of Lagrange multiplier $\xi(t)$ in the Allen-Cahn equation is to change the asymptotic constant values (± 1) of the phase function ϕ so as to conserve the volume fraction (3). In practice, the $\xi(t)$ in Eq. (3) is modified as $\xi(t)(1 - \phi^2)$ because this will keep the maximal principle for ϕ . The new Lagrange multiplier can be calculated by using the following formula

$$\xi(t) = \int_{\Omega} f(\phi) dx / \int_{\Omega} (1 - \phi^2) dx.$$

Writing the above Eqs (8)–(11) in conservative form as:

$$Q_{\tau} + I_m Q_t + (E - E_v)_x + (F - F_v)_y = S_{int}, \quad (14)$$

with,

$$\mathbf{Q} = \begin{pmatrix} p \\ u \\ v \\ \phi \end{pmatrix}, \quad \mathbf{E} = \begin{pmatrix} \beta u \\ u^2 + p \\ uv \\ u\phi \end{pmatrix}, \quad \mathbf{F} = \begin{pmatrix} \beta v \\ uv \\ v^2 + p \\ v\phi \end{pmatrix},$$

$$\mathbf{I}_m = \begin{pmatrix} 0 & 0 & 0 & 0 \\ 0 & 1 & 0 & 0 \\ 0 & 0 & 1 & 0 \\ 0 & 0 & 0 & 1 \end{pmatrix},$$

and

$$\mathbf{E}_v = \begin{pmatrix} 0 \\ \mu u_x \\ \mu v_x \\ \gamma \phi_x \end{pmatrix}, \quad \mathbf{F}_v = \begin{pmatrix} 0 \\ \mu u_y \\ \mu v_y \\ \gamma \phi_y \end{pmatrix},$$

$$\mathbf{S}_{int} = \begin{pmatrix} 0 \\ -\lambda \phi_x (\phi_{xx} + \phi_{yy}) \\ -\lambda \phi_y (\phi_{xx} + \phi_{yy}) - g(\rho_1 - \rho_2)\left(\frac{1+\phi}{2}\right) \\ \gamma(1 - \phi^2)\left(\frac{\phi}{\eta^2} + \xi(t)\right) \end{pmatrix},$$

with initial and boundary conditions given in Eq (12) and Eq (13). Here Q is the solution vector, u and v are Cartesian velocity components, p is the redefined pressure, γ represents the phase variable of the species, β is the artificial compressibility factor, τ is the

pseudo-time and t is the physical time. The I_m is singular matrix (we called it modified identity matrix) which comes when we write conservative form of our governing Eqs. (8)–(11) and we change I_m to I to remove the non-singularity and to make the diagonalization possible (more details are given in Ref. 26). S_{int} is the contribution from the capillary effect and the nonlinear terms in the phase field equation. Subscripts τ , t , x , y represent partial derivatives. The Jacobian

matrices of inviscid flux vectors \mathbf{E} and \mathbf{F} are given by \mathbf{A} and \mathbf{B} respectively as follows:

$$\mathbf{A} = \frac{\partial \mathbf{E}}{\partial \mathbf{Q}} = \begin{bmatrix} 0 & \beta & 0 & 0 \\ 1 & 2u & 0 & 0 \\ 0 & v & u & 0 \\ 0 & \phi & 0 & u \end{bmatrix},$$

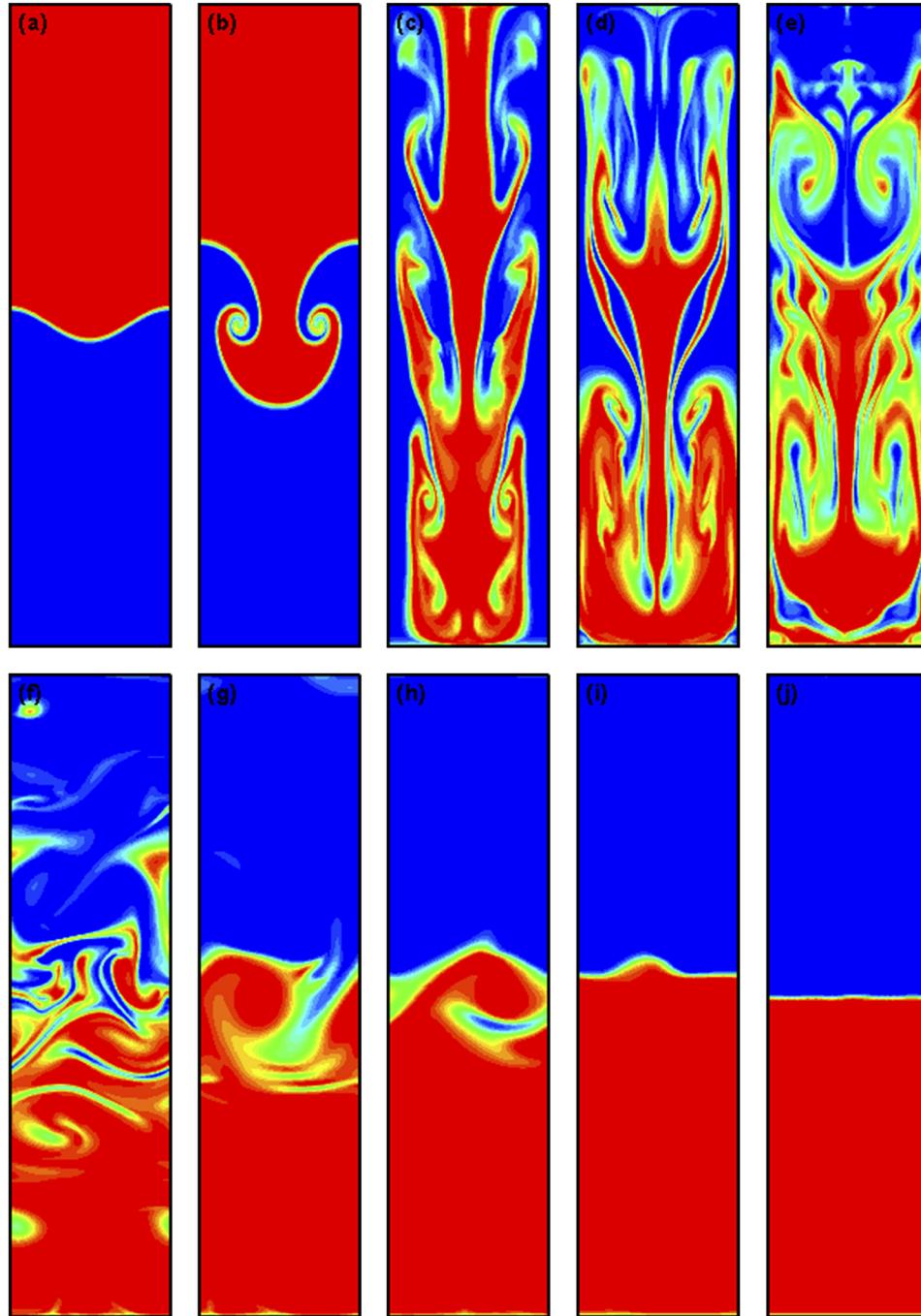


FIG. 2. Penetration of heavier fluid into lighter one at $t=0, 0.5, 1.5, 1.7, 4.5, 5.5, 7, 9, 11, 30$.

$$\mathbf{B} = \frac{\partial \mathbf{F}}{\partial \mathbf{Q}} = \begin{bmatrix} 0 & 0 & \beta & 0 \\ 0 & v & u & 0 \\ 1 & 0 & 2v & 0 \\ 0 & 0 & \phi & v \end{bmatrix}.$$

\mathbf{A}_v and \mathbf{B}_v defined in Eq. (15) are the Jacobian matrices of viscous flux vectors \mathbf{E}_v and \mathbf{F}_v respectively, which will be used in the approximate factorization scheme are

$$\begin{aligned} \mathbf{A}_v &= \frac{\partial \mathbf{E}_v}{\partial \mathbf{Q}} = \text{diag}(0, \mu, \mu, \gamma) \partial_x, \\ \mathbf{B}_v &= \frac{\partial \mathbf{F}_v}{\partial \mathbf{Q}} = \text{diag}(0, \mu, \mu, \gamma) \partial_y. \end{aligned} \quad (15)$$

\mathbf{A} and \mathbf{B} can be diagonalized as

$$\mathbf{A} = \mathbf{X} \Lambda_A \mathbf{X}^{-1},$$

$$\mathbf{B} = \mathbf{Y} \Lambda_B \mathbf{Y}^{-1},$$

where, Λ_A and Λ_B are diagonal matrices that contains the eigenvalues of matrices \mathbf{A} and \mathbf{B} respectively. The phase-field model Eq (11) for two-phase incompressible viscous flows has received a lot of attention recently and some authors^{28,33–38} among others have developed different numerical methods to solve this type of coupled system of equations.

For simulation of the results, the numerical scheme developed by Shah and Yuan²⁰ is used.

III. NUMERICAL RESULTS

In the following section, we analyzed the Rayleigh-Taylor instability phenomena for two immiscible incompressible fluids having different densities $\rho_2 = 3$, $\rho_1 = 1$ and same viscosities. We choose $\beta = 200$, $\eta = 0.01$, $\gamma = 0.000333$, $\lambda = 0.000333$ and $Re = 3000$ which are the artificial compressibility parameter, interfacial width, elastic relaxation time and surface tension coefficient respectively. The time step is taken as $\Delta t = 0.01$, the grids size is 201×401 , the initial profile is taken as $\phi(x, 0) = \tanh(\frac{y - (2+0.1 \cos(2\pi x))}{\sqrt{2}\eta})$ while periodic boundary condition in x-direction and Neumann boundary condition in the y-direction are used.

A. Rayleigh-Taylor instability along a vertical channel

In our first example, the computational domain is of size $[0, 1] \times [0, 4]$. Initially in Fig. (2)(a) at $t = 0$, the small enough initial perturbation in flow can be described by a smooth function. As the time passes in Figs. (2)(b–h), the disturbance in flow from smooth to turbulent growth has been observed (at $t = 0.5$ to $t = 9$). We also observed the transition of a single finger into spike with mushroom like shape along with some breakup and penetration of heavier fluid into the lighter one. These breakups which seems at $t = 1.5$ vanishes as time proceed as in $t = 7$, showing the phenomena of Rayleigh-Taylor instability. Here, the smaller vertices that separates absorbed completely into the fluid. At $t = 5.5$ and $t = 9$, it is clear that the falling fluid is rolled up. In our result, finally the heavier fluid has settled down completely at $t = 30$ similar to that in Ref. 21.

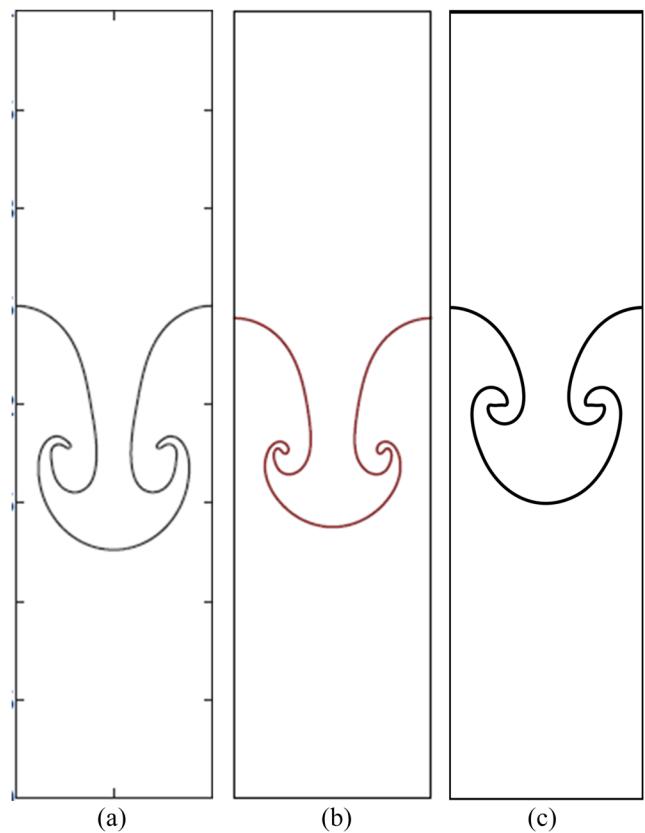


FIG. 3. Comparison of bubbles and spikes.

15 July 2023 18:51:49

The qualitative comparison of the evolution of bubble and spike positions is compared with Chiu¹⁷ and Lee¹⁸ in Fig. (3). We have observed the appearance of bubbles and spike at $t = 0.6$ whereas in Chiu¹⁷ spikes were observed at $t = 1.5$ and for Lee¹⁸ at $t = 1.75$.

Further, in Fig. (4) for lower Reynold No ($Re = 500$ and 1000), there is no roll up, while for higher Reynold No ($Re = 1000$ and 3000) the appearance of bubbles and spikes were observed resulting in the turbulence behavior of the two-phase flow.

B. Rayleigh-Taylor instability along a horizontal channel

In this section, we have conducted the same experiment along horizontal channel by using same fixed parameters and dimensions $[0, 4] \times [0, 2]$. It can be seen clearly that the primary and secondary vertices are observed turning fingers into spikes then into mushroom shapes at $t = 0.6$, $t = 0.8$ and $t = 1.0$ in Figs. (5)(b–d). Breakups and penetration of heavier fluid into lighter one is observed at $t = 1.3$, and $t = 4.0$ in Figs. (5)(e–g). At $t = 7.0$ and $t = 29$ represented in Figs. (5)(h–i) heavier fluid has fallen down completely. We have simulated our computation for long-time and compared our results with the one found in literature.¹⁸

Further more, we have shown a more detailed view of the plume at $t = 0.8$ given in Fig. (6)(a). In this case, circular shaped counter

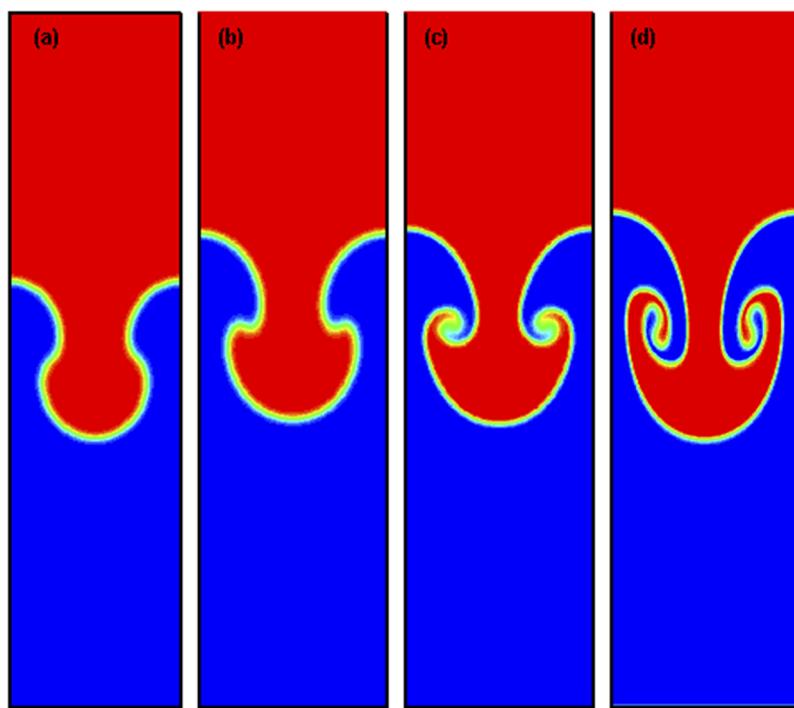


FIG. 4. Penetration of heavier fluid into lighter one at $Re=50$, 100 , 1000 , 3000 for $t=0.5$.

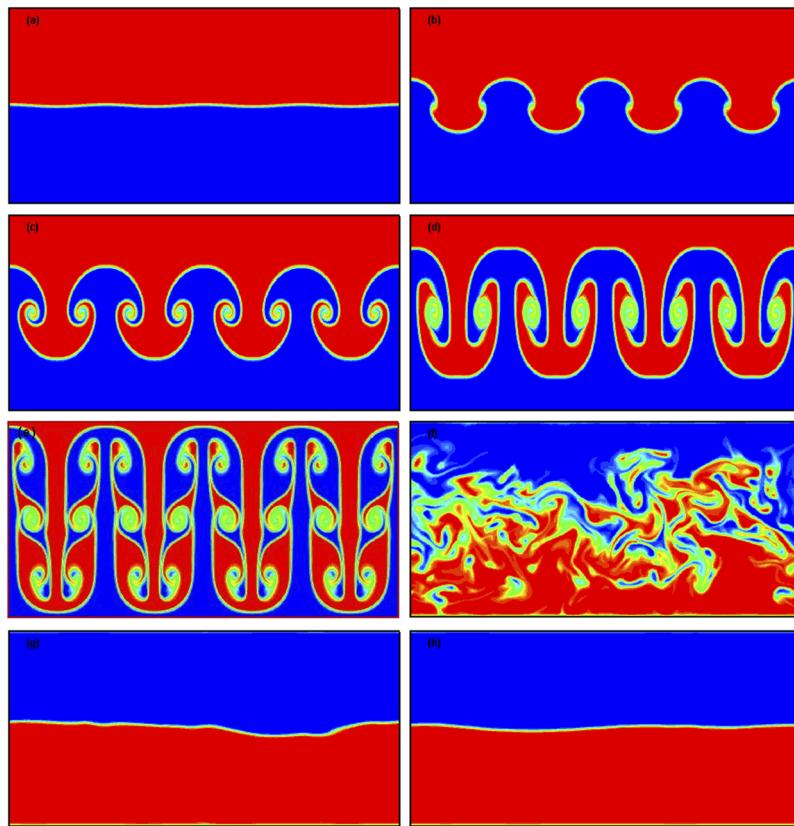
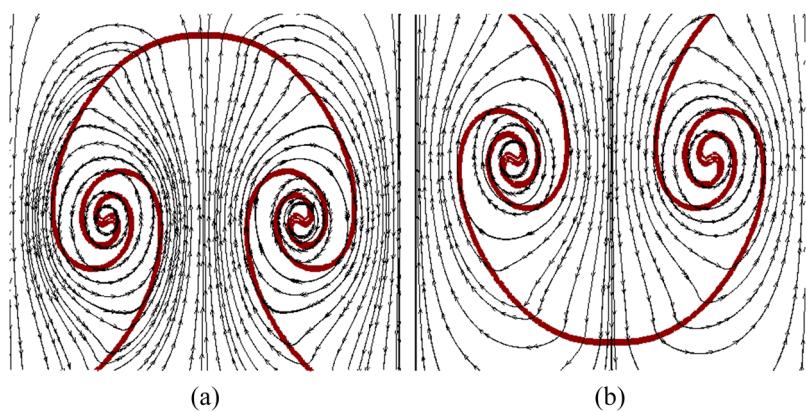


FIG. 5. Penetration of heavier fluid into lighter one at $t=0$, 0.6 , 0.8 , 1.0 , 1.7 , 4 , 7 , 30 .

FIG. 6. Streamline contours of Fig. 5(c) at $t = 0.8$.

vertices can be seen at the corners of the falling fluid. In Fig. (6)(b), however, the growth of plume is in downward direction but apparently here is no difference in the formation of circular shaped vertices in both figures (a and b).

IV. CONCLUSION

In this paper, we have successfully simulated the long-time evolution of the Rayleigh-Taylor instability problem by solving the coupled system of incompressible Navier-Stokes and phase-field equations numerically. Both Neumann and periodic boundary conditions are implemented. To deal with variable density problem, we added the Boussinesq approximation term in the momentum equation to relax the complexity of variable density formulation. Steady state solutions are computed and illustrated graphically. Future work includes the study of the three-dimensional problems having large density ratio using adaptive moving grids strategies.

REFERENCES

- ¹J. Boussinesq, *Theorie analytique de la chaleur* (Gauthier-Villars, Paris, 1903), vol. 2.
- ²N. Vladimirova and R. Rosner, “Model flames in the Boussinesq limit, the case of pulsating fronts,” *Phys Rev E* **71**, 067303-1–067303-4 (2005).
- ³Lord Rayleigh, “Investigation of the character of the equilibrium of an incompressible heavy fluid of variable density,” *Proc Lond Math Soc* **14**, 170–177 (1883).
- ⁴G. Taylor, “The instability of liquid surfaces when accelerated in a direction perpendicular to their planes. I,” *Proc R Soc Lond A* **201**, 192–196 (1950).
- ⁵S. Atzeni and J. Meyer-Ter-Vehn, *The physics of inertial fusion: beam plasma interaction, hydrodynamics, hot dense matter* (Oxford University Press, Oxford, USA, 2004).
- ⁶L. Debnath, *Nonlinear water waves* (Academic press, Boston, 1994).
- ⁷J. R. Buchler, M. Livio, and S. A. Colgate, “Supernova explosions—the role of a Rayleigh-Taylor instability,” *Space Sci Rev* **27**, 571–577 (1980).
- ⁸G. R. Baker, D. I. Meiron, and S. A. Orszag, “Boundary integral methods for axisymmetric and three-dimensional Rayleigh-Taylor instability problems,” *Physica D* **12**, 19–31 (1984).
- ⁹X. Liu, Y. Li, J. Glimm, and X. L. Li, “A front tracking algorithm for limited mass diffusion,” *J Comput Phys* **222**, 644–653 (2007).
- ¹⁰H. Terashima and G. Tryggvason, “A front-tracking/ghost-fluid method for fluid interfaces in compressible flows,” *J Comput Phys* **228**, 4012–4037 (2009).
- ¹¹C. W. Hirt and B. D. Nichols, “Volume of fluid (VOF) method for the dynamics of free boundaries,” *J Comput Phys* **39**, 201–225 (1981).
- ¹²V. R. Gopala and W. BGMvan, “Volume of fluid methods for immiscible-fluid and free-surface flows,” *Chem Eng J* **141**, 204–221 (2008).
- ¹³M. Raessi, J. Mostaghimi, and M. Bussmann, “A volume-of-fluid interfacial flow solver with advected normals,” *Comput Fluids* **39**, 1401–1410 (2010).
- ¹⁴M. Herrmann, “A balanced force refined level set grid method for two-phase flows on unstructured flow solvergrids,” *J Comput Phys* **227**, 2674–2706 (2008).
- ¹⁵T. W. H. Sheu, C. H. Yu, and P. H. Chiu, “Development of a dispersively accurate conservative level set scheme for capturing interface in two-phase flows,” *J Comput Phys* **228**, 661–686 (2009).
- ¹⁶H. Ding, P. D. M. Spelt, and C. Shu, “Diffuse interface model for incompressible two-phase flows with large density ratios,” *J Comput Phys* **226**, 2078–2095 (2007).
- ¹⁷P.-H. Chiu and Y.-T. Lin, “A conservative phase field method for solving incompressible two-phase flows,” *J Comput Phys* **230**, 185–204 (2011).
- ¹⁸H. G. Lee, K. Kim, and J. Kim, “On the long time simulation of the Rayleigh-Taylor instability,” *Int J Numer Methods Eng* **85**, 1633–1647 (2011).
- ¹⁹J. Kim, “A diffuse-interface model for axisymmetric immiscible two-phase flow,” *Appl. Math. Comput.* **160**, 589–606 (2005).
- ²⁰A. Shah and L. Yuan, “Numerical solution of a phase field incompressible two-phase flows based on artificial compressibility,” *Computer and fluids* **42**, 54–61 (2011).
- ²¹J. Kim, “Phase-field models for multi-component fluid flows,” *Communications in Computational Physics* **12**(3), 613–661 (2012).
- ²²J. D. van der Waals, “The thermodynamic theory of capillarity under the hypothesis of a continuous variation of density,” *Journal of Statistical Physics* **20**(2), 200–244 (1979).
- ²³J. W. Cahn and J. E. Hilliard, “Free energy of a nonuniform system. I. Interfacial free energy,” *J. Chem. Phys.* **28**, 258–267 (1958).
- ²⁴Y. N. Di, R. Li, and T. Tang, “General moving mesh framework in 3D and its application for simulating the mixture of multi-phase flows,” *Commun. Comput. Phys* **3**(3), 582–602 (2008).
- ²⁵A. J. Chorin, “A numerical method for solving incompressible viscous flow problems,” *Journal of Computational Physics* **2**, 12–26 (1967).
- ²⁶A. Shah, S. Saeed, and L. Yuan, “An artificial compressibility method for 3D phase-field model and its application to two-phase flows,” *International Journal of Computational Methods* **14**(5), 1750059 (2017).
- ²⁷H. G. Lee and J. Kim, “A comparison study of the Boussinesq and the variable density models on buoyancy-driven flows,” *Journal of Engineering Mathematics* **75**(1), 15–27 (2012).
- ²⁸Z. Tan, K. M. Lim, and B. C. Khoo, “An adaptive mesh redistribution method for the incompressible mixture flows using phase-field model,” *J. Comput. Phys.* **225**, 1137–1158 (2007).
- ²⁹G. Tegze, T. Pusztai, and L. Granasy, “Phase-field simulation of liquid phase separation with fluid flow,” *Mater. Sci. Eng. A* **413**, 418–422 (2005).

- ³⁰H. G. Lee, "High-order and mass conservative methods for the conservative Allen-Cahn equation," *Computers and Mathematics with Applications* **72**, 620C631 (2016).
- ³¹A. Shah, M. Sabir, M. Qasim, and P. Bastain, "Efficient numerical scheme for solving the Allen-Cahn equation," *Numer Methods Partial Differential Eq* **34**, 1820–1833 (2018).
- ³²A. Shah, M. Sabir, and S. Ayub, "An adaptive time-stepping scheme for numerical solution of Cahn-Hilliard equation with variable mobility," *Journal of Applied Mathematics and Mechanics* **99**, e201800246 (2019).
- ³³X. F. Yang, C. Liu, and J. Shen, "Numerical simulations of jet pinching-oil and drop formation using an energetic variational phase-field method," *J. Comput. Phys* **218**, 417–428 (2006).
- ³⁴Y. N. Di, R. Li, and T. Tang, "General moving mesh framework in 3D and its application for simulating the mixture of multi-phase flows," *Commun, Comput. Phys.* **3**(3), 582–602 (2008).
- ³⁵C. Liu and J. Shen, "A phase-field model for the mixture of two incompressible fluids and its approximation by a Fourier-spectral method," *Physica D* **179**, 211–228 (2003).
- ³⁶P. Yue, J. J. Feng, C. Liu, and J. Shen, "Difuse-interface simulations of drop coalescence and retraction in viscoelastic fluids," *J. Non-Newtonian Fluid Mech* **129**, 163–176 (2005).
- ³⁷Z. Zhang and H. Tang, "An adaptive phase-fileld method for the mixture of two incompressible fluids," *Comput. Fluids* **36**, 1307–1318 (2007).
- ³⁸Y. Sun and C. Beckermann, "Sharp interface tracking using the phase-field equation," *J. Comput. Phys* **220**, 626–653 (2007).